EUROPEAN ORGANIZATION FOR NUCLEAR RESEARCH

CERN-EP/85-04
14 January 1985

OBSERVATION OF ANOMALOUS SCALING VIOLATION IN MUON PAIR PRODUCTION BY 194 GeV/c π^--TUNGSTEN INTERACTIONS

NA10 COLLABORATION

CERN[1]-Naples[2]-Ecole polytechnique[3]-Strasbourg[4]-ETH[5]

B. Betev[1a], J.J. Blaising[4b], P. Bordalo[3], A. Boumediene[3], L. Cerrito[3], A. Degré[4b], A. Ereditato[2], S. Falciano[5c], K. Freudenreich[1], E. Gorini[2], M. Guanziroli[5], H. Hofer[5], P. Juillot[4], L. Kluberg[3], P. Lecomte[5], P. Le Coultre[5], R. Morand[4b], B. Mours[4b], A. Romana[3], R. Salmeron[3], P. Strolin[2], H. Suter[5], V.L. Telegdi[5], J. Varela[3d], G. Viertel[5], J. Wallace-Hadrill[1] and M. Winter[4]

ABSTRACT

The differential cross-section for dimuon production by 194 GeV/c π^- on W, as measured by the NA10 Collaboration, is compared with theoretical models. The wide kinematical range of the data, extending well above the Υ resonances, provides the opportunity of a comparison with 'realistic' Drell-Yan models, i.e. with those allowing for scaling violation in the hadronic structure functions. The data in fact clearly indicate the failure of the 'naïve' Drell-Yan model, while the available 'realistic' versions (leading logarithm approximation and next-to-leading logarithm approximation in first order QCD), although giving a better description of the data, still disagree in the x_F and $\sqrt{\tau}$ dependences of the cross-section at high dimuon masses. This disagreement is referred to here as 'anomalous' scaling violation. The dependence of the results on external inputs (nucleon and pion-sea structure functions) is analysed; it is shown that in the next-to-leading logarithm approximation the value $\langle K \rangle = 1.03 \pm 0.03$ (stat.) can be obtained for the ratio experimental/theoretical cross-section.

(Submitted to Zeitschrift für Physik)

1 CERN, Geneva, Switzerland.
2 University of Naples and INFN, Naples, Italy.
3 Ecole polytechnique, Palaiseau, France.
4 CRN and University Louis Pasteur, Strasbourg, France.
5 ETH, Zurich, Switzerland.
a. Permanent address: Institute for Nuclear Research and Nuclear Energy, Sofia, Bulgaria.
b. Now at LAPP, Annecy-le-Vieux, France.
c. Now at INFN, Sezione di Roma, Italy.
d. Now at Centro de Fisica da Materia Condensada, Lisbon, Portugal.

1. INTRODUCTION

In the preceding paper [1] we reported the results of a measurement of the differential cross-section for the production of high-mass muon pairs by a 194 GeV/c π^- beam on a tungsten target. In the present article we compare these results with current theoretical predictions.

The main features of lepton pair production in hadronic collisions have been explained in the framework of the Drell–Yan model [2], in which a quark of one of the hadrons annihilates with an antiquark of the other hadron, producing a virtual photon which materializes into a lepton pair. However, in the region where they were sensitive, i.e. below the Υ resonance, past experiments [3] have already shown that, for a variety of incident particles and for different energies, the total muon pair production cross-section is larger than the one computed according to the original Drell–Yan model. Their ratio, the so-called 'K-factor', was assumed to be a constant, with a measured value of 2.3 ± 0.5 [4].

The original Drell–Yan model, henceforth referred to by us as 'naïve', has to be amended to include QCD corrections. These have been computed perturbatively to lowest order in $\alpha_s(M^2)$, with the following results:

a) In the leading logarithm approximation (LLA) [5], one simply has to allow for the 'evolution' of the hadron structure functions, well known (for nucleons) from the observed scaling violations in deep inelastic scattering (DIS). Quantum chromodynamics (QCD) provides, through the Altarelli–Parisi equations [6], a procedure for calculating this evolution;
b) The next-to-leading logarithm approximation (NLLA) [7] predicts essentially the same $\sqrt{\tau}$ and x_F dependences as the LLA, but supplies an overall scale factor of about 1.8.

The Drell–Yan model calculated with allowance for scaling violation might be called a 'realistic' one. Obviously, it will lead to differences in the $\sqrt{\tau}, x_F$ distribution as compared to its 'naïve' precursor. The predicted differences are, however, small in the kinematical region covered by earlier experiments [3] (i.e. *below* the Υ), thereby justifying the extraction of the structure functions from the data in the framework of the 'naïve' model, especially in the cases of limited statistics.

The high statistics of our experiment and the fact that it provides data above the Υ (i.e. at high values of τ) call for a comparison with 'realistic' models. For a differential comparison, it is useful to introduce a K-function, defined by:

$$d\sigma^{exp}/dx_F \,|_{\sqrt{\tau}} = K(x_F,\sqrt{\tau})\, d\sigma^{th}/dx_F \,|_{\sqrt{\tau}}\,, \tag{1}$$

where $d\sigma^{exp}/dx_F$ is the experimentally determined cross-section, and $d\sigma^{th}/dx_F$ the corresponding theoretical one, both at the same value of $\sqrt{\tau}$. Should theory and experiment disagree only in absolute magnitude, then this K-function would be a constant, i.e. become the usual K-factor mentioned above. The theoretical cross-section obviously depends on the model assumed and on the numerical values taken for the pion and nucleon structure function parameters.

2. FORMALISM

In the 'naïve' Drell–Yan formalism the differential cross-section may be written as

$$d^2\sigma/dx_1dx_2 = (4\pi\alpha^2/9M^2) \sum_i e_i^2 \,[q^i_{H_1}(x_1) \cdot \bar{q}^i_{H_2}(x_2) + (1 \leftrightarrow 2)]\,, \tag{2}$$

where M is the dimuon mass, x_1 and x_2 are the fractional momenta of the hadrons H_j carried by the quarks of flavour i, $q^i_{Hj}(\bar{q}^i_{Hj})$ is the density of quark (antiquark) i in hadron H_j, e_i is the quark (antiquark) electric charge; the factor 1/3 is incorporated for colour conservation. Denoting the total energy by $\sqrt{s}$ and the dimuon longitudinal momentum by P_L^* in the centre-of-mass system, one has

$$\tau = x_1 \cdot x_2 = M^2/s\,, \qquad x_F = x_1 - x_2 = 2P_L^*/\sqrt{s}\,. \tag{3}$$

The quark densities in equation (2) are defined as the sum of valence and sea densities by relations of the type

$$\begin{aligned} \bar{q}^u_\pi(x) &= V_\pi(x) + S_\pi(x)\,, \quad (x = x_1) \\ q^u_P(x) &= u(x) + S_P(x)\,, \quad (x = x_2)\,, \\ &\ldots \end{aligned} \tag{4}$$

The pion structure functions, assumed to be SU(2) symmetrical for the valence quarks and SU(3) symmetrical for the sea quarks, are parametrized according to Buras and Gaemers [8]:

$$xV_\pi(x) = A_v x^{\alpha_\pi}(1-x)^{\beta_\pi} \quad \text{for the valence quarks}$$

and (5)

$$xS_\pi(x) = A_s(1-x)^{\gamma_\pi} \quad \text{for the sea quarks}$$

with the normalizations:

$$\int_0^1 V_\pi(x)\,dx = 1 \quad \text{and} \quad \int_0^1 x[2V_\pi(x) + 6S_\pi(x)]\,dx = 1 - \langle g_\pi \rangle \quad \text{at } M = M_0\,, \tag{6}$$

where $\langle g_\pi \rangle$ represents the fractional momentum carried by the gluons. For the nucleon structure functions we use the following parametrization:

$$xu(x) = A_u x^{\alpha_1}(1-x)^{\beta_v}(1+\gamma x^{\alpha_2})$$

and

$$xd(x) = A_d x^{\alpha_1}(1-x)^{\beta_v+1}(1+\gamma x^{\alpha_2}) \text{ for the valence quarks} \tag{7}$$

and

$$xS_p(x) = x\bar{u}(x) = x\bar{d}(x) = 2x\bar{\lambda}(x) = C(1-x)^{\beta_s} \quad \text{for the sea quarks}\,.$$

The normalization coefficients for the valence quarks are again obtained by quark counting:

$$\int_0^1 u(x)\,dx = 2\,, \quad \int_0^1 d(x)\,dx = 1\,. \tag{8}$$

For the 'realistic' Drell–Yan model (in the LLA approximation) as already referred to in the Introduction, one simply has to replace the scale-independent densities by M^2-dependent ones in Eq. (2). In the framework of the parametrizations (5) and (7), scaling violation implies that the parameters α_π, α_1, etc., evolve with $\bar{s}$, for example:

$$\alpha_1 = \alpha_1(\bar{s}) \quad \text{with } \bar{s} = \ln\left[\ln(M^2/\Lambda^2)/\ln(M_0^2/\Lambda^2)\right]\,. \tag{9}$$

Conversely, one recovers the 'naïve' Drell–Yan model by fixing the parameters at some specific M^2.

3. COMPARISON WITH MODELS, AND PION VALENCE STRUCTURE FUNCTION

The data analysed here were taken with the NA10 spectrometer which is described elsewhere [9]. We analysed a sample of 155,000 events with masses greater than 4.07 GeV/c^2. Their x_1,x_2 distribution is shown in Fig. 1. The region of the Υ resonances is excluded from the analysis by omitting events with masses between 8.5 and 11 GeV/c^2.

We shall consider successively the predictions of the 'naïve' and of the 'realistic' Drell–Yan models. For each model, we shall first determine the pion valence parameters, then compute the corresponding theoretical cross-section, and finally study the $\sqrt{\tau}$ and x_F dependence of $K(x_F,\sqrt{\tau})$ as defined by Eq. (1). As external inputs, we use parameters given in Table 1, i.e. for the *nucleon* those obtained by Eisele [10] by fitting the parametrization (7) to the most recent CDHS neutrino data in iron [11], and for the *pion* sea those obtained by the NA3 Collaboration from their independent measurements with π^+ and π^- beams [4].

We start with the 'naïve' Drell–Yan model, fixing the nucleon parameters at $M^2 = 25\ (\text{GeV})^2$, and assuming the validity of this model over the whole kinematical domain where we have reliable data, i.e. $\sqrt{\tau} > 0.24$ and $x_F > 0$. The resulting fitted values are shown in Table 2. It is evident from the value of χ^2 that this model, as could be expected, gives a poor fit. To establish the detailed nature of the discrepancy, we compare (see Fig. 2) the theoretically predicted cross-section, scaled with $\langle K \rangle$, in four successive $\sqrt{\tau}$ bins with the experimental points. It is clear that the disagreement is most pronounced in the highest $\sqrt{\tau}$ bin, which contributes excessively to the overall χ^2, while affecting the values of the fitted parameters only little. An alternative representation of the same fit is given in Fig. 3 in terms of the K-function, Eq. (1).

Both representations indicate that the 'naïve' Drell–Yan prediction, even when multiplied by a constant, fails to reproduce the data over the entire mass range covered by the NA10 experiment. This is not too astonishing in view of the fact that scaling violation (in the nucleon) is well established through DIS experiments, and shows the usefulness of a K-function in place of a constant K-factor. As displayed in Fig. 3, the local K-factors $\bar{K}$ decrease with increasing $\sqrt{\tau}$; note that almost all points in the top $\sqrt{\tau}$ bin lie below the $\langle K \rangle$ averaged over the lower bins. This is qualitatively what known scaling violation predicts.

For a comparison of our results with those of NA3 we have adopted the same external parameters as used in Ref. [4] and determined the pion valence parameters in the same kinematical range ($x_F > 0$ and $0.24 < \sqrt{\tau} < 0.42$), obtaining $\alpha_\pi = 0.41 \pm 0.03$, $\beta_\pi = 1.11 \pm 0.4$,

and $\langle K \rangle = 2.36 \pm 0.11$ (statistical errors). These values are in good agreement with those of Ref. [4].

We then proceed to the comparison with the 'realistic' Drell-Yan model in the LLA. Here the pion valence parameters were determined with two alternative approaches:

a) In one approach, the pion valence parameters at a given mass were calculated using the entire data set and taking into account the known M^2-dependence of the structure functions. This calculation was performed parametrizing the pion structure evolution in a form suggested by Buras and Gaemers [12]

$$\alpha_\pi(M^2) = \alpha_{\pi 0}(M_0^2) + \alpha_{\pi 1} \cdot \bar{s} \quad \text{and} \quad \beta_\pi(M^2) = \beta_{\pi 0}(M_0^2) + \beta_{\pi 1} \cdot \bar{s}\,, \tag{10}$$

with $\bar{s}$ as defined in Eq. [9].

Constraining the moments of the pion structure function by the Altarelli-Parisi equations, we obtained a set of relations expressing $\alpha_{\pi 1}$ and $\beta_{\pi 1}$ as functions of $\alpha_{\pi 0}$ and $\beta_{\pi 0}$, given the above M^2 dependence. We obtained the values listed in Table 2 and the cross-section shown in Fig. 2. The dependence of $K(x_F,\sqrt{\tau})$ on x_F is shown in Fig. 4 in the four $\sqrt{\tau}$ intervals.

b) In another approach, we started with the values $\alpha_{\pi 0}$ and $\beta_{\pi 0}$, as determined according to the 'naïve' Drell-Yan model in the interval $0.24 < \sqrt{\tau} < 0.30$, then computed the M^2-dependence of the pion structure functions, solving the Altarelli-Parisi equations directly, as described by Gabellini et al. [13]. Thus knowing the mass dependence of the pion valence structure function we computed the cross-section [Eq. (2)]. The corresponding K-function is within the errors identical with that obtained by the method described in (a).

The shapes of the predicted x_F distributions are with this 'realistic' model closer to the observed ones (see the improved χ^2 in Table 2), but the disagreement persists at high $\sqrt{\tau}$. Furthermore, a disagreement between the model and the data can also be observed (see Fig. 5) in the behaviour of $K(\sqrt{\tau},x_F)$ integrated with respect to x_F.

It is *a priori* clear that including the next-to-leading logarithm terms of the first-order approximation (NLLA) should not allow the explanation of the observed disagreement, since according to Kubar et al. [7] these additional terms should practically not change the $\sqrt{\tau}$ and x_F dependence of the differential cross-section in our kinematical region. Nevertheless, we have adjusted $\alpha_{\pi 0}$ and $\beta_{\pi 0}$ to our data in the framework of their calculation. The values of the fitted pion parameters are again listed in Table 2. As expected, the magnitude of the predicted differential cross-section is closer to the observed one, and the predicted shape shows the same type of disagreement with experiment as in the case of LLA (see Fig. 6).

It is evident both from qualitative considerations on the anticipated evolution of the structure functions as well as from the curves in Fig. 2 that scaling violation should play but a minor role for $\sqrt{\tau} < 0.42$, i.e. below the Υ. It is therefore of some interest to fit the data with $\sqrt{\tau} < 0.42$, so as to be able to estimate the likelihood that the measured points in the top $\sqrt{\tau}$ bin of Fig. 2 are consistent with the model predictions; the resultant parameters are included in Table 2. For this estimate (in NLLA), we adopt the uncertainty in the predicted cross-section (or K-function) as indicated by the shaded band (one standard deviation) in Fig. 2. This band allows only for the uncertainties in the pion structure function parameters, i.e. neglects those due to the nucleon. The top bin contributes 19 to the total χ^2 of 56, corresponding for the 6 degrees of freedom involved to a confidence level (C.L.) of 3‰.

There is another interesting conclusion to be drawn from our fits. While scaling violation in the nucleon has been well established by DIS, there is a lack of any direct *experimental* evidence to date for the analogous effect in the pion. In order to display our sensitivity to the M^2-dependence in the pion, we have performed an analysis allowing only for the nucleon's evolution. While the χ^2 below the Υ is still good, one obtains an even worse χ^2 for the prediction for the top bin, as can be seen from the corresponding entry in Table 2. Since the 'realistic' models are unable to reproduce our data where evolution matters, this result provides only circumstantial evidence on the evolution of the pion structure function.

4. SENSITIVITY OF THE K-FUNCTION TO THE EXTERNAL PARAMETERS

The comparison of our cross-section with QCD predictions in the NLLA shows a disagreement in shape for $\sqrt{\tau} > 0.54$, as well as a disagreement in the overall absolute normalization [$\langle K \rangle = 1.58 \pm 0.07$ (stat.)]. We shall first investigate the influence of the choice of the nucleon parameters on the disagreement in shape observed in the region above the Υ's.

Since Ref. [10] does not attach errors to the parameters, this influence cannot be assessed quantitatively, i.e. by appropriately increasing the width of the standard-deviation error band in Fig. 2. However, we have attempted to estimate it qualitatively by comparing differential cross-sections calculated in LLA with nucleon structure functions determined from fits to the data from two *different* ν–DIS experiments [11,14]. In these calculations [15], we adopted for the nucleon the sea of Ref. [10] and the valence parametrization of Buras–Gaemers as given in Table 1. With these inputs we fitted, as in the previous cases, for the pion valence parameters and the K-factor. The results, for the CCFRR nucleon [14], are summarized in Table 3. In the top bin above the Υ's, the renormalized $d\sigma/dx_F$'s so computed and scaled with $\langle K \rangle$ differ only by 7% to 1% as x_F goes from 0 to 0.5. The smallness of these differences is due to the fact that the changes are predominantly absorbed by the K-factor and by the pion structure function parameters. Apart from the question of the proper choice of the nucleon valence parameters, there is also that concerning the Fermi motion. In fact, our data [1] are corrected for the latter while those obtained in DIS experiments [11,14] make no special allowance for it. The nucleon parameter changes that correspond to such a correction are, however, smaller than those between fits to Refs. [11] and [14], and would again be absorbed by the pion parameters. Attributing the observed behaviour of K in the top $\sqrt{\tau}$ bin to uncertainties in the nucleon structure function alone seems thus unlikely in view of this analysis.

We next turn to the absolute normalization. While the statistical error on $\langle K \rangle$ is small (6%), large systematic uncertainties (see Tables 2 and 3) arise mainly from three sources: i) errors (9%) in the luminosity and collection efficiency of our set-up [1]; ii) differences in the fits to the two DIS neutrino experiments [11,14] we have considered (20%); iii) errors in the pion sea parameters [4] (25%). We estimated the last error by allowing a variation in the parameters γ_π and g_π by one standard deviation, and by duly accounting for correlations. In view of these uncertainties, our result for $\langle K \rangle$ is compatible with the QCD predictions in the NLLA.

It is worth stressing that by adopting the parametrization [15] of the ν-data of Ref. [14] and by fixing the values $\gamma_\pi = 6.3$ and $g_\pi = 0.32$ (both well within the quoted errors of Ref. [4]) one obtains, in NLLA, the value $\langle K \rangle = 1.03 \pm 0.03$ (stat.), i.e. remarkable agreement between this QCD approximation and experiment.

It is also possible to determine the value of $\langle K \rangle$ by a method which altogether avoids the uncertainties due to the pion sea. It suffices to determine the pion valence parameters, and hence $\langle K \rangle$, in a τ-range where the pion sea contribution is negligible. Such a range is $0.36 < \sqrt{\tau} < 0.42$, where we have 12,000 events. The results are included in Table 4, and the value for $\langle K \rangle = 1.39 \pm 0.39$ (stat.) (nucleon of Refs. [10,11]), is in good agreement with the above consideration.

As already explained in Ref. [9], we have checked the sensitivity of our results to various other inputs, and found the experimental inefficiencies to be small. Biases related to the model used for the Monte Carlo simulation were also investigated. They lead only to corrections well within the statistical errors.

5. CONCLUSION

A very large sample of dimuon events, provided by the NA10 experiment allowed a differential analysis over a wide kinematical region extending well beyond the Υ resonances and leads to the following conclusions:

i) For $\sqrt{\tau} < 0.42$, i.e. below the Υ, our results are in good agreement with those of previous experiments [4], if analysed with the same external inputs.

ii) According to the choice of the nucleon-structure functions, $\langle K \rangle$ (defined with respect to the NLLA) varies between 1.34 and 1.58, and the 25% uncertainty due to the parameters of the pion sea makes these values well consistent with the theoretical prediction ($\langle K \rangle \simeq 1$).

iii) For $\sqrt{\tau} > 0.54$, i.e. for masses above the Υ's:

a) conventional scaling does not predict $d\sigma/dx_F$ correctly, i.e. one observes, at a C.L. of 3×10^{-3}, a disagreement with the data;

b) $K(\sqrt{\tau})$ cannot be described over the entire $\sqrt{\tau}$ range by a single K-factor.

We refer to these observations as *anomalous* scaling violation.

iv) Above $\sqrt{\tau} = 0.54$, qualitative evidence for the evolution of the pion structure function is obtained.

One may speculate on the origin of the scaling anomalies that we are observing. The importance of the higher-order QCD corrections [16] which have yet to be computed is an open question. The correctness of the factorization approach, and in particular its interdependence on the P_T distributions (over which we integrate!), is also subject to critical discussion. It might be worth noting that the A-dependence of the nucleon structure function, known as the EMC effect [17], does not supply a valid explanation of the observed anomalies: allowing for such an effect between iron and tungsten [18] in hadronic muon-pair production leads to a much smaller effect than reported here.

REFERENCES

[1] B. Betev et al., preceding paper.

[2] S.D Drell and T.M. Yan, Phys. Rev. Lett. **25** (1970) 316, and Ann. Phys. **66** (1971) 578.

[3] R. Barate et al., Phys. Rev. Lett. **43** (1979) 1541;
J. Badier et al., Phys. Lett. **89B** (1979) 145;
M. Corden et al., Phys. Lett. **96B** (1980) 417;
A.S. Ito et al., Phys. Rev. **23D** (1981) 604.

[4] J. Badier et al., Z. Phys. C, Particles and Fields, **18** (1983) 281.

[5] For a review, see G. Altarelli, Phys. Rep. **81** (1982) 1.

[6] G. Altarelli and G. Parisi, Nucl. Phys. **B126** (1977) 298.

[7] J. Kubar et al., Nucl. Phys. **B175** (1980) 251.

[8] A.J. Buras, Nucl. Phys. **B125** (1977) 125.

[9] L. Anderson et al., Nucl. Instrum. Methods **223** (1984) 26.

[10] P. Eisele, private communication.

[11] H. Abramovicz et al., Z. Phys. C, Particles and Fields, **17** (1983) 283.

[12] A.J. Buras and K.J.F. Gaemers, Nucl. Phys. **B132** (1978) 249.

[13] Y. Gabellini et al., Nucl. Phys. **B211** (1983) 509.

[14] D. MacFarlane et al. (CCFRR Collaboration), Fermi Lab.-Pub 83/108 Exp. (1983).

[15] M. Winter, Thesis, CRN and University of Strasbourg, France, in preparation.

[16] A study including soft gluon effects is being prepared by a group from the University of Nice, France — Y. Gabellini et al.

[17] J.J. Aubert et al., Phys. Lett. **123B** (1983) 275.

[18] R.G. Arnold et al., SLAC-PUB-3320, April 1984 (T/E).

Figure captions

Fig. 1 : Distribution of events in the x_1–x_2 plane.

Fig. 2 : Comparison of the measured cross-sections with various model calculations and scaled with the appropriate $\langle K \rangle$.

DY = 'naïve' Drell–Yan,

LLA = leading logarithm approximation,

NLLA = next-to-leading logarithm approximation.

The pion valence parameters were adjusted over the entire data sample, i.e. $0.24 \leq \sqrt{\tau} \leq 0.42$ and $0.54 \leq \sqrt{\tau} \leq 0.72$, in the cases of DY and LLA; in the case of NLLA, they are adjusted in the region $0.24 < \sqrt{\tau} < 0.42$. The uncertainty in the predicted cross-sections induced by the errors in the fitted pion parameters is illustrated (for the NLLA model) by the shaded area in the graph for the highest $\sqrt{\tau}$ bin.

Fig. 3 : Variations of the K-function defined with respect to the 'naïve' Drell–Yan model. The pion valence parameters have been adjusted over the entire data sample. The dashed line represents the average $\langle K \rangle$ factor obtained in the fit. The mean values of $\bar{K}$ corresponding to individual τ-bins are indicated numerically.

Fig. 4 : Variations of the K-function with respect to the LLA predictions. The dashed line represents the average $\langle K \rangle$ factor obtained in the fit. The mean values of $\bar{K}$ corresponding to individual τ-bins are indicated numerically.

Fig. 5 : Variations of the K-function $K(\sqrt{\tau})$, integrated for $0.0 < x_F < 0.5$, as a function of $\sqrt{\tau}$ in the LLA model.

Fig. 6 : Variations of the K-function with respect to the NLLA calculation. The mean values of $\bar{K}$ corresponding to individual τ-bins are indicated numerically.

Table 1

External inputs. For the definition of the parameters see Eqs. (7), (8), and (10) of the text.

Nucleon Parameters

	Refs. 10,11	Refs. 14,15
α_1	$0.3543 + 0.4122\ \bar{s}$	$0.6190 - 0.1678\ \bar{s}$
α_2	$1.5760 + 2.0170\ \bar{s}$	———
β_V	$3.8330 + 2.8680\ \bar{s}$	$2.8670 + 0.6687\ \bar{s}$
γ_V	11.57	0.00
β_S	$7.417 - 1.138\bar{s} + 13.22\bar{s}^2 - 4.966\bar{s}^3 - 1.86\bar{s}^4$	As Ref. 10
C	$(0.50758 + 0.23006\bar{s} + 0.067345\bar{s}^2)\ /\ 2.8$	As Ref. 10
M_0^2 [GeV^2/c^4]	5.0	5.0
Λ [GeV/c^2]	0.30	0.30

Pion Parameters

A_1	B_1	C_1	A_2	B_2	C_2	γ_π	$\langle g_\pi \rangle$	M_0^2 [GeV^2/c^4]	Λ [GeV/c^2]
0.0579	−0.2370	−0.0328	0.5150	−0.0114	0.0544	8.4	0.47	25.0	0.3

$$\alpha_{\pi 1} = A_1 + B_1\,\alpha_{\pi 0} + C_1\,\beta_{\pi 0} \qquad \beta_{\pi 1} = A_2 + B_2\,\alpha_{\pi 0} + C_2\,\beta_{\pi 0}$$

Table 2

Results of fits of pion valence parameters, at $M_0^2 = 25\ GeV^2$, for different model assumptions.
$\langle K \rangle$ is the mean normalization factor between data and model resulting from the fits.
Nucleon structure parameters are from Refs. [10,11]; pion sea parameters are those of Ref. [4].
HYBR = pion structure functions without evolution. Only statistical errors are given.

Fit region : $0.24 < \sqrt{\tau} < 0.72$									
Model	α_0	α_1	β_0	β_1	K−factor	χ^2/d.o.f.	Confidence level (%)	χ^2 (below ϒ)	χ^2 (above ϒ)
DY [10,11]	0.44±0.03	———	1.18±0.04	———	2.60±0.11	199.2/42	0.0	83.7	115.6
LLA [10,11]	0.39±0.02	−0.07±0.01	0.98±0.04	0.56±0.002	2.78±0.12	56.0/42	7.1	37.4	18.6
NLLA [10,11]	0.40±0.03	−0.07±0.01	1.03±0.04	0.57±0.002	1.61±0.07	57.5/42	5.3	36.4	21.2
HYBR [10,11]	0.44±0.03	———	1.13±0.04	———	2.62±0.12	53.0/42	11.8	28.4	24.6
Fit region : $0.24 < \sqrt{\tau} < 0.42$									
Model	α_0	α_1	β_0	β_1	K−factor	χ^2/d.o.f.	Confidence level (%)	χ^2 (below ϒ)	χ^2 (above ϒ)
DY [10,11]	0.41±0.03	———	1.09±0.04	———	2.71±0.13	75.3/36	0.0	75.3	134.8
LLA [10,11]	0.41±0.03	−0.07±0.01	1.02±0.04	0.57±0.002	2.69±0.12	36.6/36	44.7	36.6	20.2
NLLA [10,11]	0.41±0.03	−0.07±0.01	1.04±0.04	0.57±0.002	1.58±0.07	36.0/36	47.4	36.0	21.7
HYBR [10,11]	0.44±0.03	———	1.14±0.04	———	2.58±0.12	28.2/36	18.1	28.2	25.0
Fit region : $0.24 < \sqrt{\tau} < 0.30$									
Model	α_0	α_1	β_0	β_1	K−factor	χ^2/d.o.f.	Confidence level (%)	χ^2 (below ϒ)	χ^2 (above ϒ)
DY [10,11]	0.42±0.05	———	1.07±0.11	———	2.67±0.21	7.1/ 7	———	———	———

Table 3

Same as Table 2, except nucleon valence parameters are from Refs. [14,15].
Nucleon sea parameters are from Refs. [10,11]. Only statistical errors are given.

Fit region : $0.24<\sqrt{\tau}<0.72$									
Model	α_0	α_1	β_0	β_1	K−factor	χ^2/d.o.f.	Confidence level (%)	χ^2 (below Υ)	χ^2 (above Υ)
LLA [14,15]	0.40±0.03	−0.07±0.01	0.96±0.04	0.56±0.002	2.33±0.10	72.3/42	0.2	43.3	29.1
NLLA [14,15]	0.41±0.03	−0.07±0.01	1.01±0.04	0.57±0.002	1.35±0.06	77.8/42	0.0	42.9	34.9
HYBR [14,15]	0.45±0.03	———	1.12±0.04	———	2.20±0.10	72.8/42	0.2	28.8	44.0
Fit region : $0.24<\sqrt{\tau}<0.42$									
Model	α_0	α_1	β_0	β_1	K−factor	χ^2/d.o.f.	Confidence level (%)	χ^2 (below Υ)	χ^2 (above Υ)
LLA [14,15]	0.42±0.03	−0.07±0.01	0.98±0.04	0.56±0.002	2.28±0.10	42.9/36	20.1	42.9	29.8
NLLA [14,15]	0.42±0.03	−0.07±0.01	1.01±0.04	0.57±0.002	1.34±0.06	42.6/36	21.2	42.6	35.5
HYBR [14,15]	0.45±0.03	———	1.11±0.04	———	2.18±0.10	28.2/36	17.9	28.2	45.3

Table 4

Pion valence parameters in NLLA, corresponding to nucleon valence structure functions of Refs. [10,11 and 14,15]. Only statistical errors are given.

Fit region : $0.36<\sqrt{\tau}<0.42$									
Model	α_0	α_1	β_0	β_1	K−factor	χ^2/d.o.f.	Confidence level (%)	χ^2 (below T)	χ^2 (above T)
NLLA [14,15]	0.42±0.14	−0.08±0.03	1.03±0.10	0.57±0.005	1.37±0.42	8.6/12	25.8	60.7	37.2
NLLA [10,11]	0.48±0.15	−0.09±0.04	1.08±0.10	0.57±0.006	1.39±0.39	8.8/12	27.5	54.5	23.2

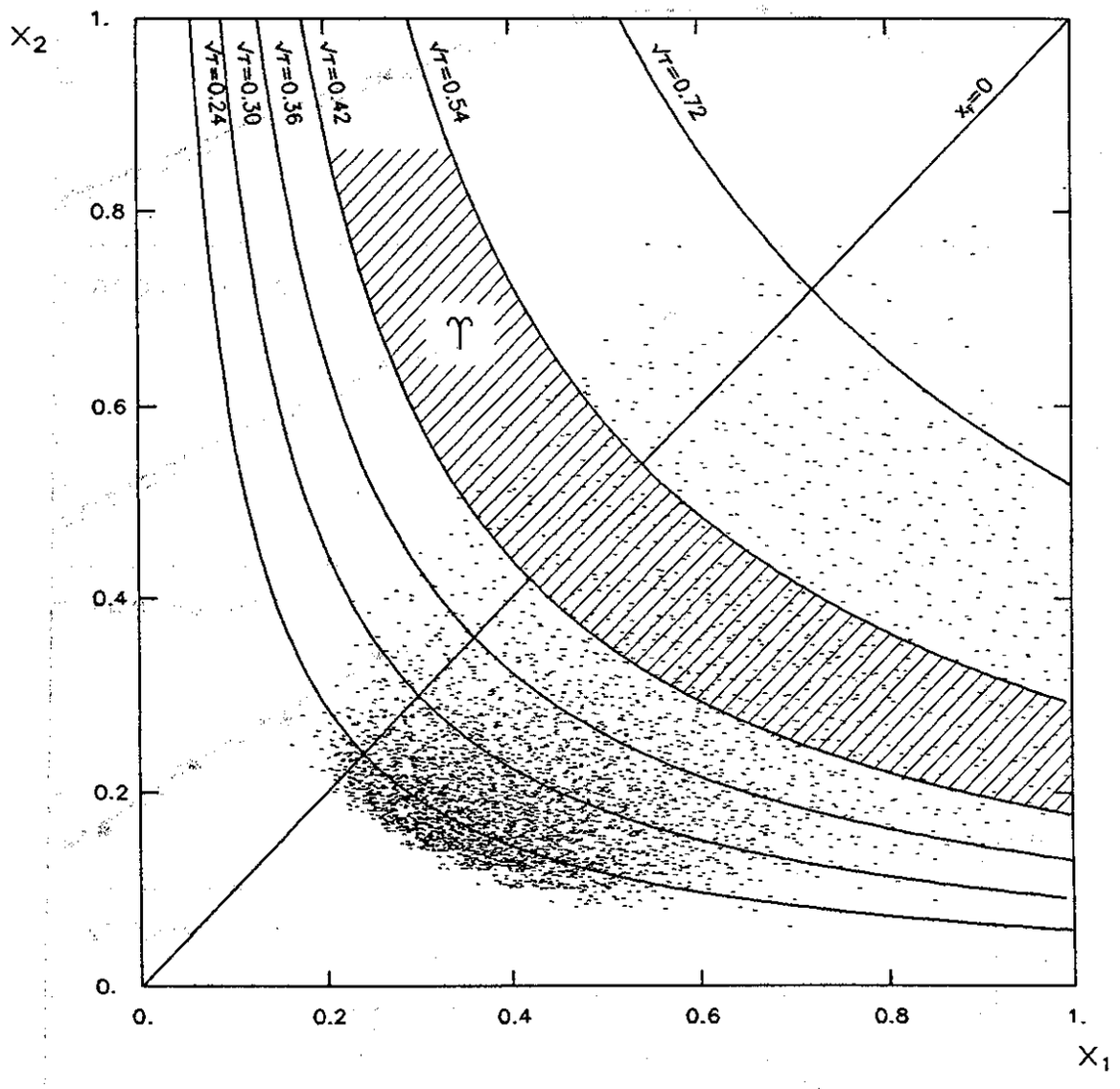
X2
1.
0.8
0.6
0.4
0.2
0.
0.
0.2
0.4
0.6
0.8
1.
X1
√τ=0.24
√τ=0.30
√τ=0.36
√τ=0.42
√τ=0.54
√τ=0.72
x=0
ϒ

Fig. 1

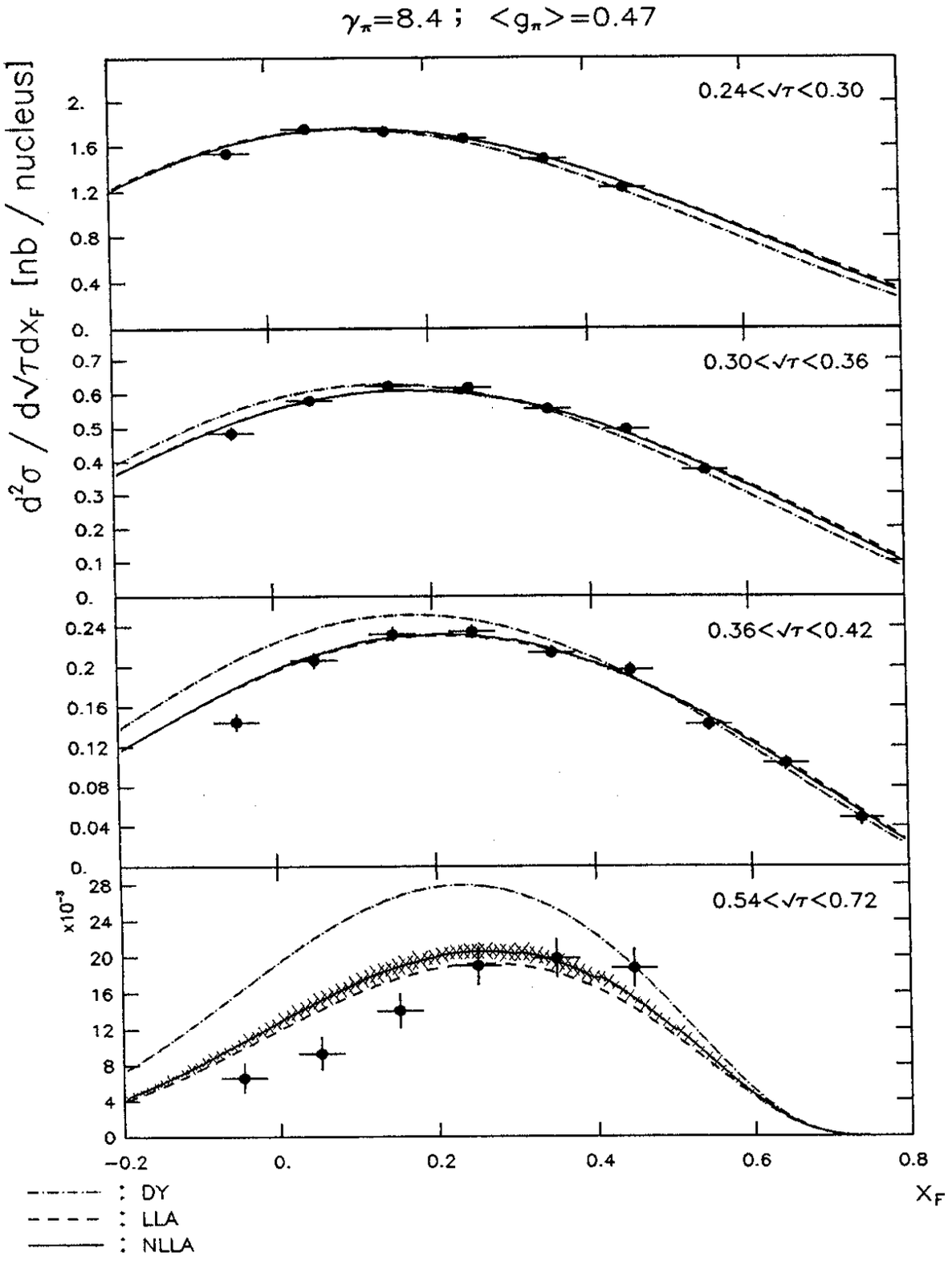
γ_π=8.4 ; $<g_\pi>$=0.47
$d^2\sigma$ / $d\sqrt{\tau}dx_F$ [nb / nucleus]
0.24<√τ<0.30
0.30<√τ<0.36
0.36<√τ<0.42
0.54<√τ<0.72
x10⁻³
X_F
: DY
: LLA
: NLLA

Fig. 2

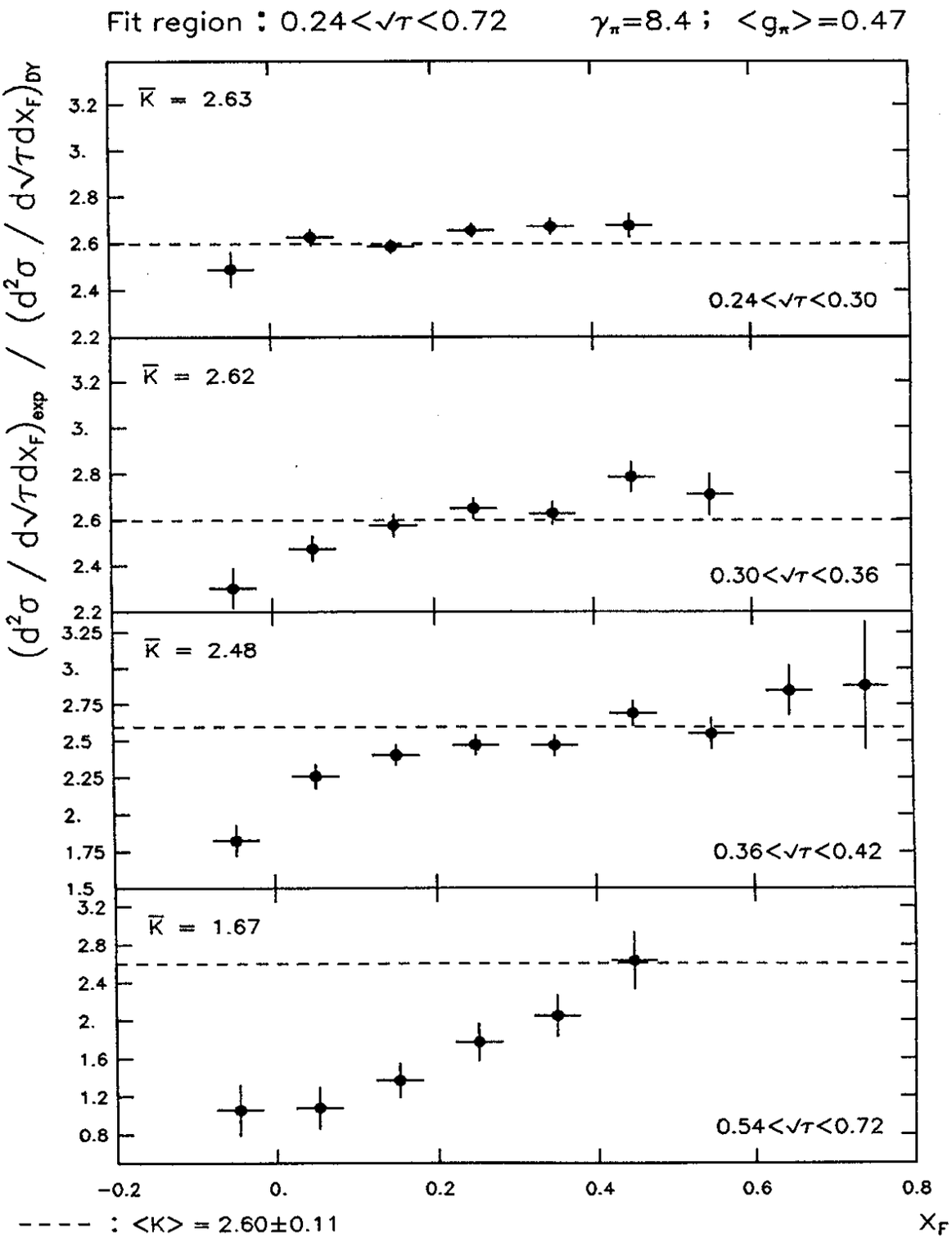
Fit region : 0.24<√τ<0.72
γ_π=8.4 ; <g_π>=0.47
$(d^2\sigma / d\sqrt{\tau} dx_F)_{exp} / (d^2\sigma / d\sqrt{\tau} dx_F)_{DY}$
$\bar{K}$ = 2.63
0.24<√τ<0.30
$\bar{K}$ = 2.62
0.30<√τ<0.36
$\bar{K}$ = 2.48
0.36<√τ<0.42
$\bar{K}$ = 1.67
0.54<√τ<0.72
---- : <K> = 2.60±0.11
x_F

Fig. 3

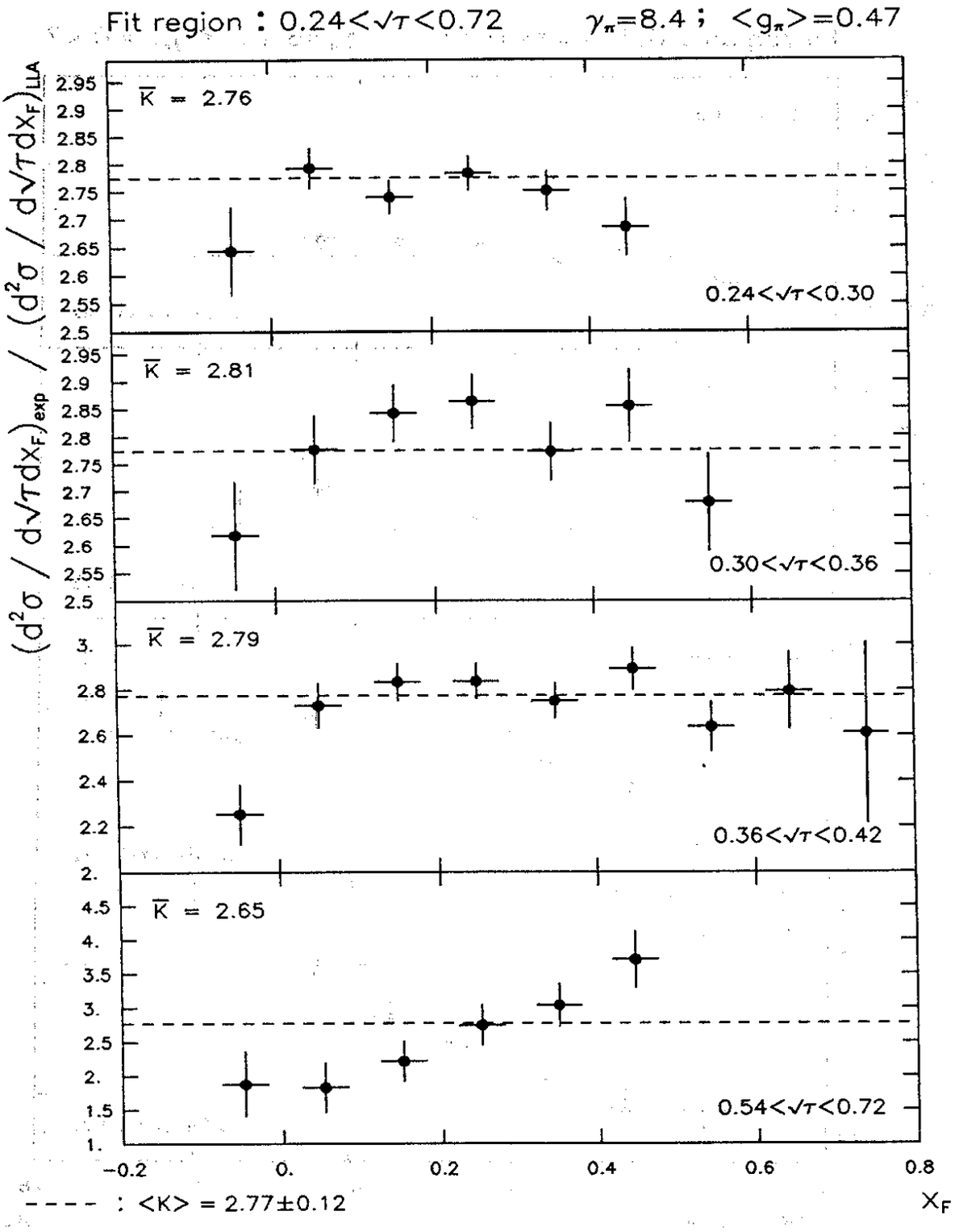
Fit region : 0.24<√τ<0.72
γπ=8.4 ; <gπ>=0.47
(d²σ / d√τdxF)exp / (d²σ / d√τdxF)LLA
K̄ = 2.76
0.24<√τ<0.30
K̄ = 2.81
0.30<√τ<0.36
K̄ = 2.79
0.36<√τ<0.42
K̄ = 2.65
0.54<√τ<0.72
---- : <K> = 2.77±0.12
XF

Fig. 4

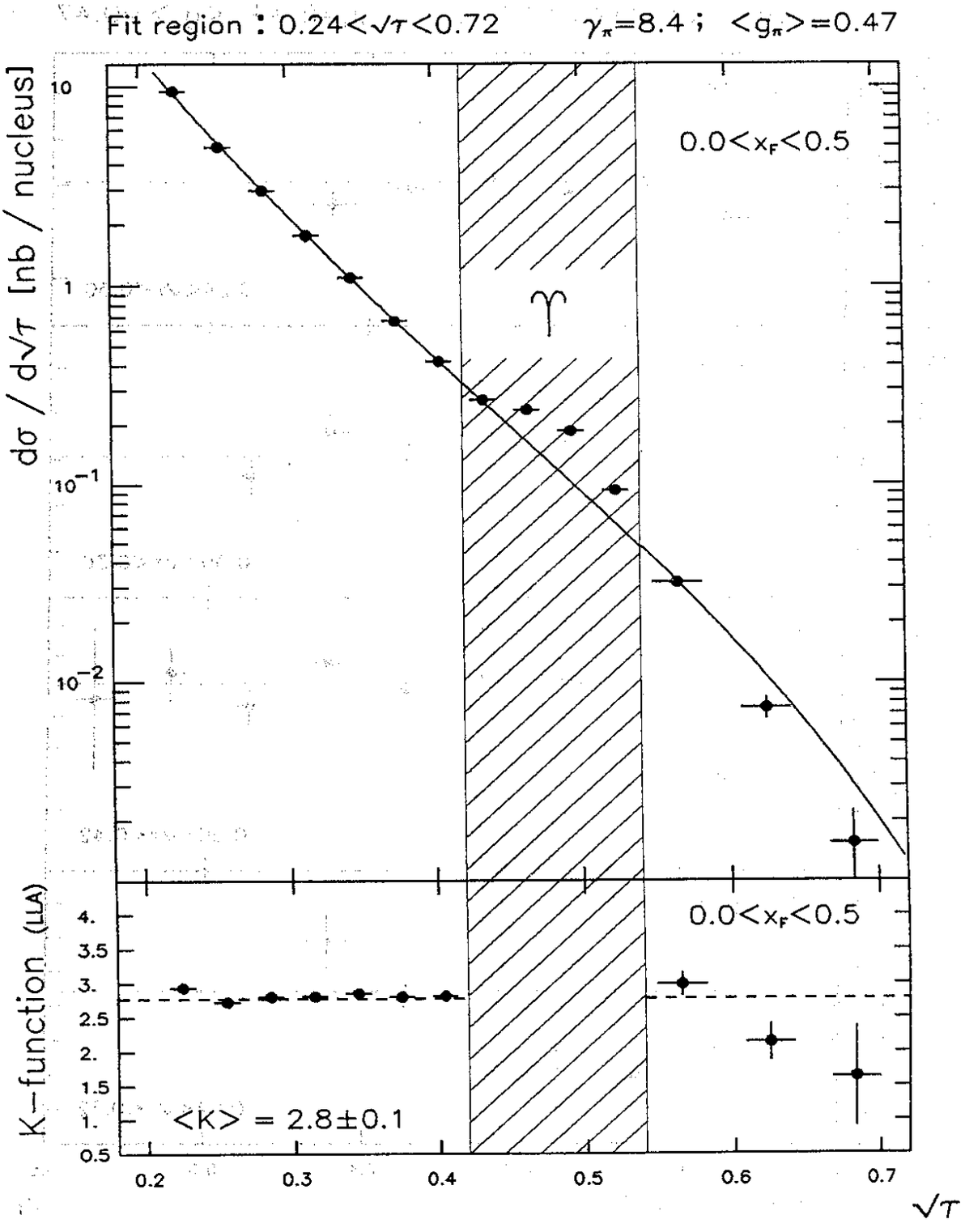
Fit region : 0.24<√τ<0.72
γπ=8.4 ; <gπ>=0.47
dσ / d√τ [nb / nucleus]
0.0<xF<0.5
Υ
K−function (LLA)
<K> = 2.8±0.1
√τ

Fig. 5

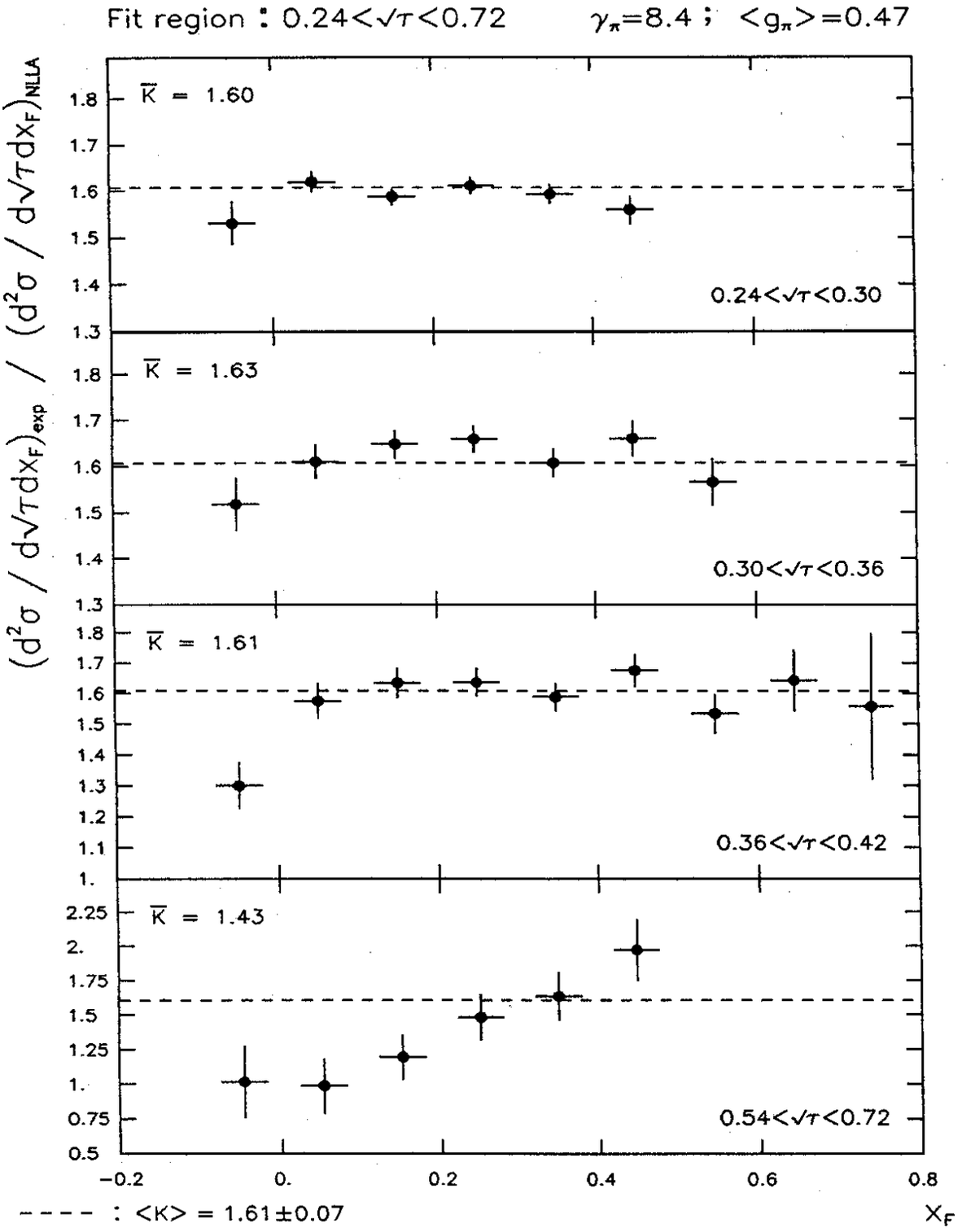
Fit region : 0.24<√τ<0.72
γ_π=8.4 ; <g_π>=0.47
$(d^2\sigma / d\sqrt{\tau}dx_F)_{exp} / (d^2\sigma / d\sqrt{\tau}dx_F)_{NLLA}$
$\bar{K}$ = 1.60
0.24<√τ<0.30
$\bar{K}$ = 1.63
0.30<√τ<0.36
$\bar{K}$ = 1.61
0.36<√τ<0.42
$\bar{K}$ = 1.43
0.54<√τ<0.72
---- : <K> = 1.61±0.07
x_F

Fig. 6